CHAPTER 5
Experimental result and discussion

5.1 Introduction

After the fabrication processes of GaAs/GaAlAs staircase bandgap photodiode have been described, the experimental results will be discussed in this chapter. These particular results are based upon the current-voltage characteristic and spectral response.

5.2 Fabricated structures

Even though we have designed and studied on several photodiode structures in chapter 3, we do not pick up all structures to fabricate. We have fabricated three structures as depicted in Fig. 5.1. These structures are similar to structure A1, A2 and A3 respectively except the thickness. Structure I and II were grown by LPE while structure III which its pn junction was formed by Zn diffusion, was grown by MBE. Therefore, the staircase bandgap structure layers of structure III are rather thin and also its junction depth depends upon the diffusion condition. Anyway, we can examine this particular junction depth by its current-voltage characteristic and also by its spectral response on the following section.

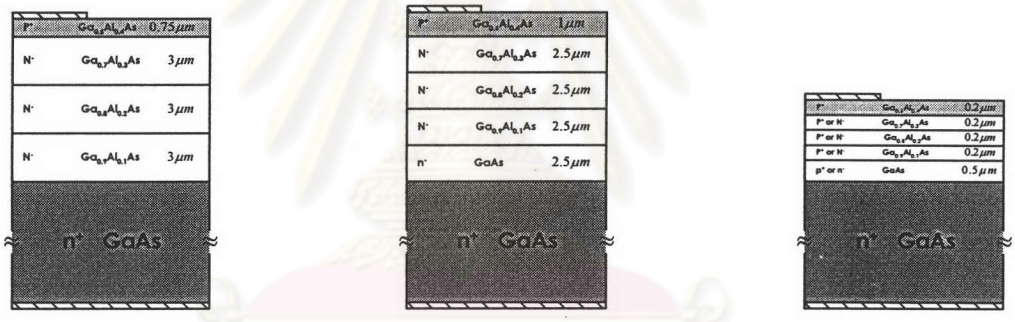

(a) Structure I **(b) Structure II** **(c) Structure III**

Fig. 5.1 Fabricated structures

5.3 Current-Voltage characteristic (IV characteristic)

After the photodiode chip is mounted on the testing house, it will be brought into connection with the curve tracer model 577-177 D2 from Tektronix for the IV characterization as shown in Fig. 5.2. The IV characteristics of structure I, II and III are depicted as in Fig. 5.3. From the intersection of the characteristic slope under forward bias condition and the horizontal axis, the cut-in voltage of structure I, II and III are 1.3 V, 1 V and 1.6 V respectively. From the N_A and N_D of the structures we can calculate the theoretical cut-in voltages of $Ga_{0.6}Al_{0.4}As$, $Ga_{0.7}Al_{0.3}As$, $Ga_{0.8}Al_{0.2}As$, $Ga_{0.9}Al_{0.1}As$ and GaAs which are 1.746 V, 1.627 V, 1.508 V, 1.389 V and 1.273 V respectively. In case of structure I and II, the pn-junction is at the interface of $Ga_{0.6}Al_{0.4}As$ and $Ga_{0.7}Al_{0.3}As$ therefore the cut-in voltage of these structures should be around 1.6 to 1.7 Volts. It is maybe because of an imperfect of the semiconductor metallurgical junction as well as its morphology. In case of structure III, we can simply analyze the junction depth from the cut-in voltage. According to the theoretical cut-in voltage, the junction depth of this structure possibly locates in between $Ga_{0.7}Al_{0.3}As$ and $Ga_{0.8}Al_{0.2}As$ region.

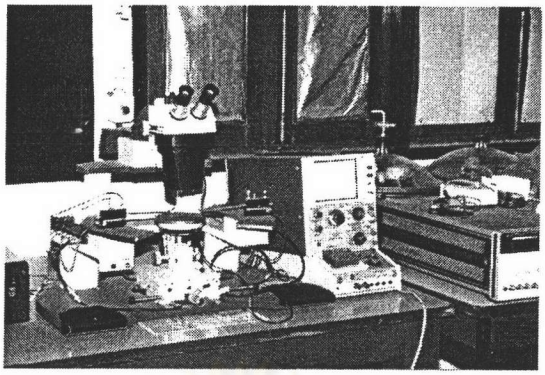

Fig. 5.2 The curve tracer and the probe station used in current-voltage characteristics measurement

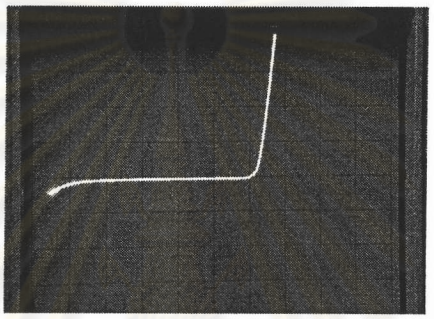

5 mA/Div
1V/Div

(a) Structure I

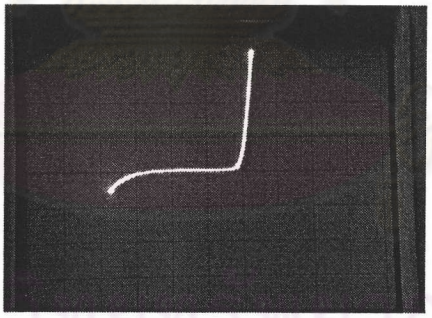

5 mA/Div
1V/Div

(b) Structure II

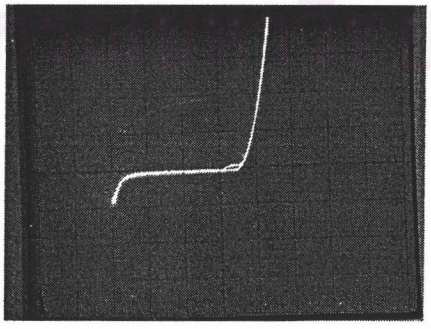

5 mA/Div
2V/Div

(c) Structure III

Fig. 5.3 IV-characteristics of (a) structure I (b) structure II and (c) structure III

Under the reverse bias condition, the breakdown voltages of structure I, II and III are 4 V, 2 V and 5 V respectively. These values are too low because of (1) the low quality of active layer (2) an imperfect of semiconductor metallurgical junction and its morphology. The breakdown voltage of the photodiodes is usually in a range of 15-20 Volts depending upon the doping concentration and the thickness of the active layer.

5.4 Spectral response

The spectral response is one of the most important characteristics in which it helps us to check the designed wavelength ranges that our photodiode responds. We can measure the spectral response by the photocurrent measurement system, which is typically composed of:

1. Tungsten lamp: used as light source
2. Lens: to align the tungsten light input to the monochromator
3. Monochromator: to select the photons of wavelength λ to impinge on the sample
4. Sample holder with bias circuit: for setting and biasing the sample
5. Digital multi-meter: for reading the photocurrent data
6. DC voltage-current source: for biasing the measured sample
7. Computer and program: for controlling the measurement system and collecting the measured data
8. Optical power meter ML9001A and optical power sensor MA9411A: for measuring the power of tungsten lamp

Firstly, we will turn on the tungsten lamp at least 1 hour before measuring its spectral characteristic for the steady state condition. The schematic of the lamp power measurement is illustrated in Fig. 5.4. After that we will setup the spectral response measurement system as depicted in Fig. 5.5. To ensure the reliability of the measurement system, we will measure the spectral response of commercial photodiode and compares to its spectral response in data sheet. The photodiode that is mounted on the testing housing is then brought into the measurement system under reverse biasing and subsequently the spectral response measurement is running from 400 nm to 900 nm by computer controlling. Finally, the measured photocurrent data is normalized by the tungsten power characteristic. Therefore we will consider the relative sensitivity curve rather than the photocurrent. The comparison between experimental and theoretical spectral response of structure I, II and III are depicted in Fig. 5.6. The discussion of these spectral responses will be reported on the following section.

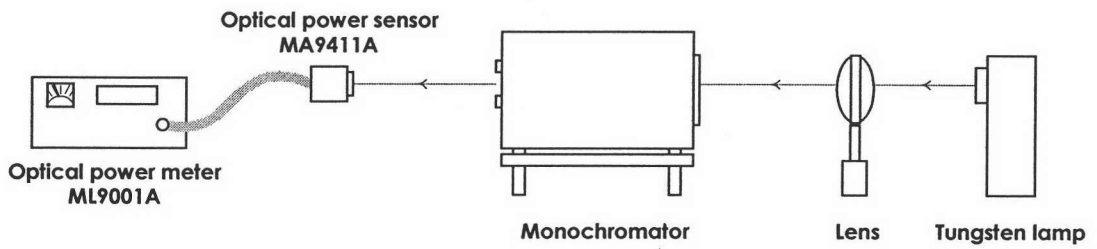

Fig. 5.4 A schematic of the lamp power measurement

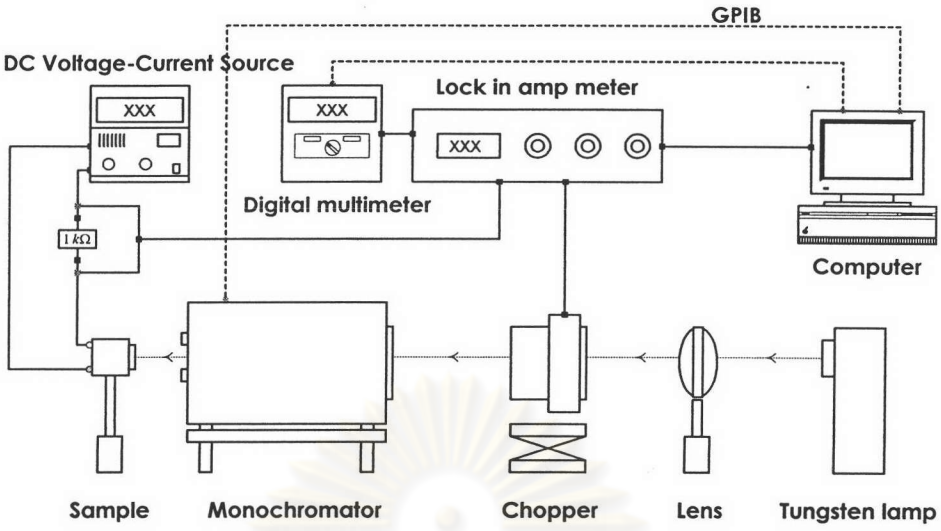

Fig. 5.5 A schematic of the spectral response measurement setup

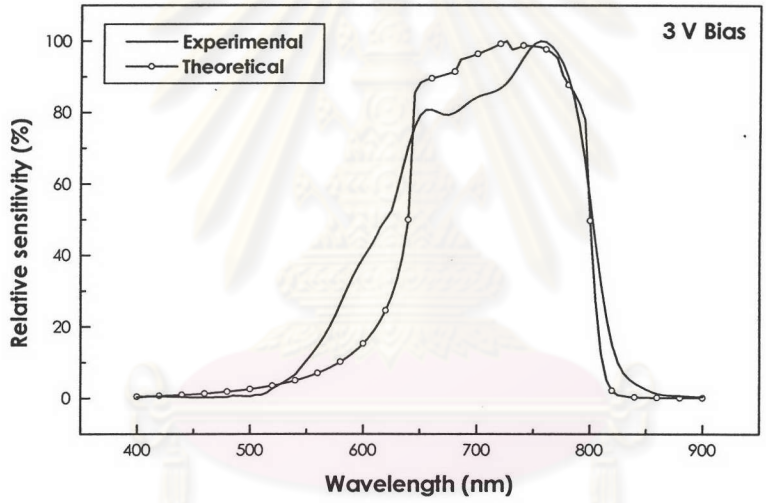

(a) Structure I

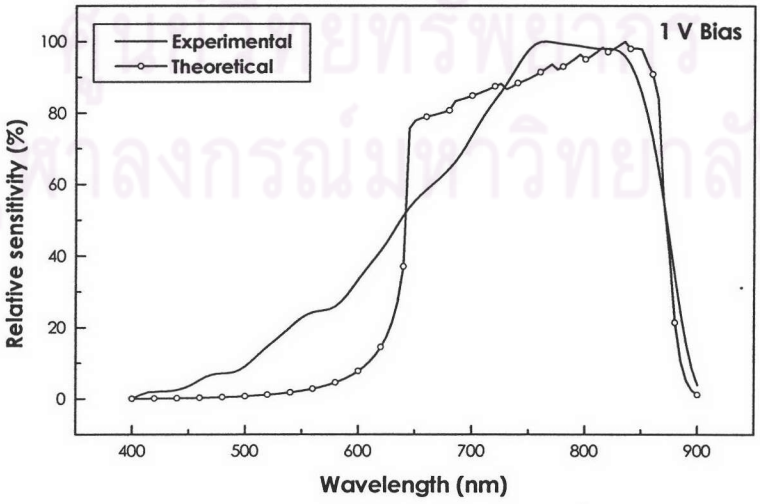

(b) Structure II

Fig. 5.6 The comparison between experimental and theoretical spectral response of (a) Structure I (b) Structure II and (c) Structure III

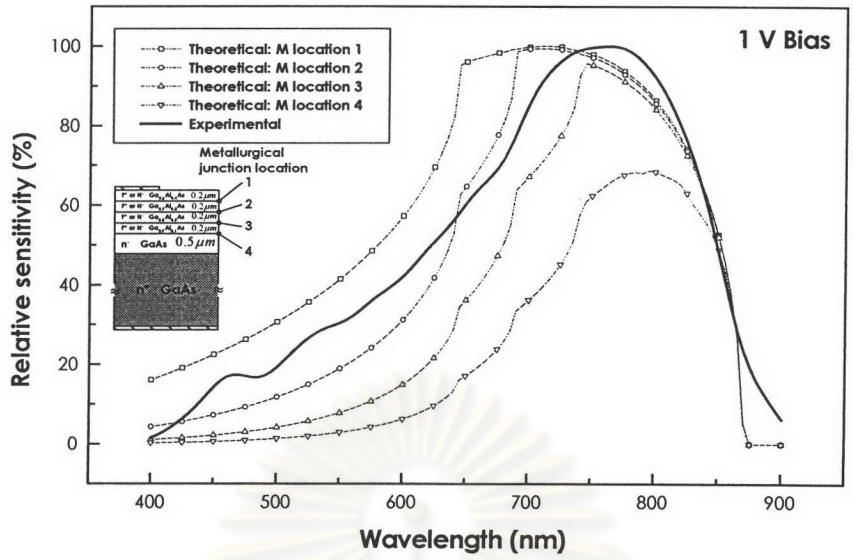

(c) Structure III

Fig. 5.6 (Continued)

5.5 Discussion

Structure I

The comparison between the experimental and theoretical spectral response of structure I is shown in Fig. 5.6 (a). In case of the experimental spectral response, it gradually rises up at wavelength nearly 520 nm until 650 nm, it fluctuates in a short range of between 650 and 680 nm before slowly increasing up to the peak at 760 nm. This fluctuation can be caused by the recombinations existing at the interfaces of active layers and nearby as illustrated in Fig. 5.7. The conduction band discontinuity would act as a well to trap electrons while the valence band discontinuity introduces the barrier to block the hole. For this reason, the generation rate would moderately decrease at the active layer interfaces and nearby. As for the case of cutoff wavelength, both are corresponded to nearly 800 nm, which is the cutoff wavelength of $Ga_{0.9}Al_{0.1}As$. It is clearly seen that the experimental spectral result is not very consistent with the theoretical one only a point that is it expands more broader especially at the short wavelengths. This is because of the diffusion current which was negligible in the calculation. To get rid of this current, the method of blocking layer will be employed into the structure. (see more detail in master thesis of Miss Duangporn Chatweerachaikit)

Structure II

The comparison between the experimental and theoretical spectral response of structure II is depicted in Fig. 5.6 (b). The experimental spectral response is slowly raised up from 400 nm to the peak at nearly 760 nm and subsequently cutoffs at nearly 870 nm, which is corresponding to the cutoff wavelength of GaAs. In the same manner, the spectral response of short wavelengths expands more broader than the theoretical one due to the diffusion current. The slightly fluctuation between 640 and 850 nm was again caused by the recombinations existing at active layer interfaces and nearby as illustrated in Fig. 5.7.

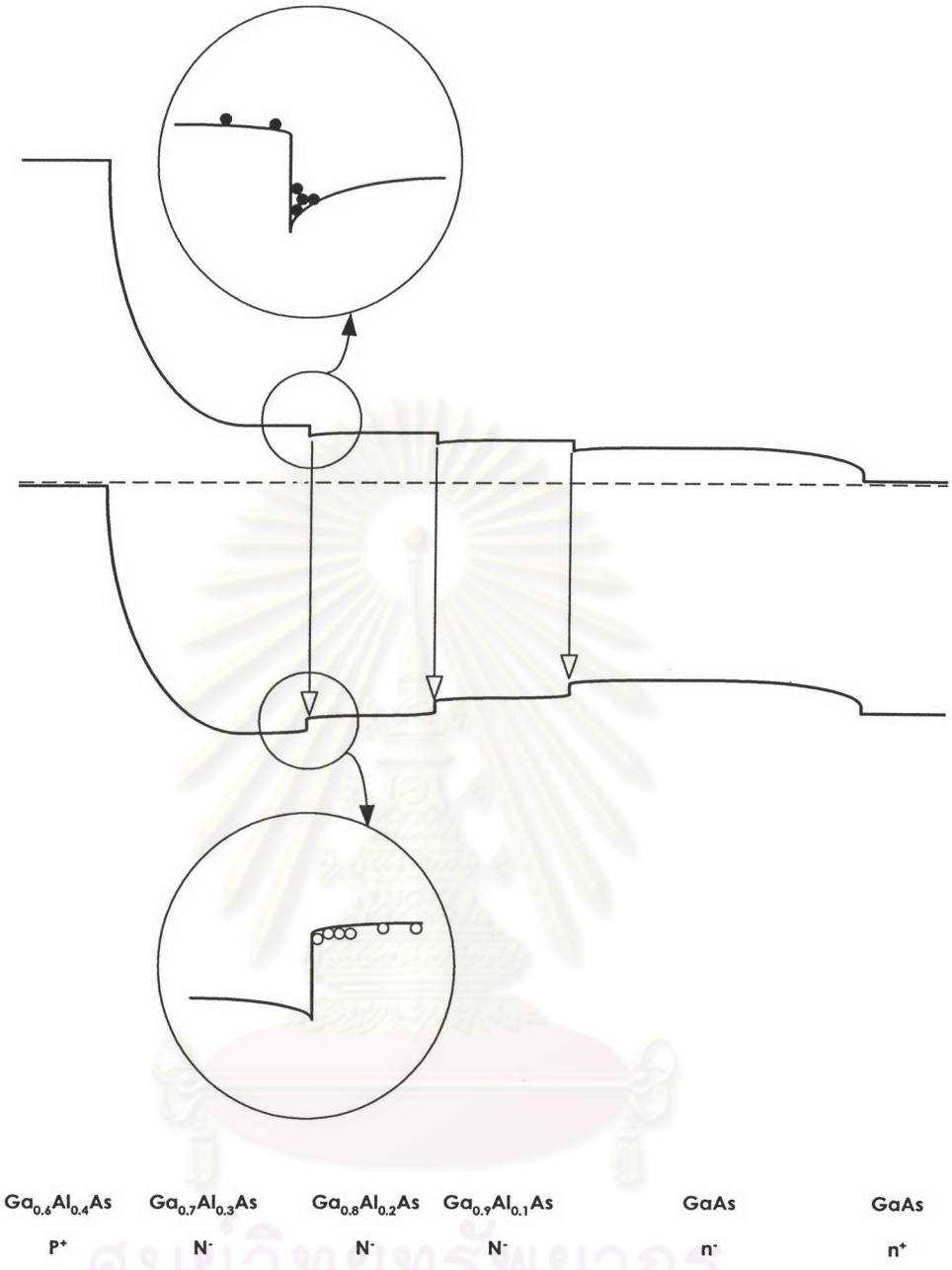

Fig. 5.7 Recombinations in active region of structure I, II and III

Structure III

In this case, the theoretical spectral response calculated with different metallurgical junction (M) locations are compared to the experimental result, as shown in Fig. 5.6 (c). It's clearly seen that the experimental spectral response is agreed with the one of the metallurgical junction location between $Ga_{0.7}Al_{0.3}As$ and $Ga_{0.8}Al_{0.2}As$ region, which is corresponding to the result analyzed by the cut in voltage that we have mentioned earlier. Our experimental result is also strongly supported by a research on spectral response of GaAs photodiodes fabricated by RTD (Rapid Thermal Diffusion) of Zn. [23] Since the pn-junction depth is controlled by the heating rate as well as the diffusion time. The deeper the junction is, the lower the spectral response exhibits at short wavelengths, as illustrated in Fig. 5.8. The problem of the diffusion current and the recombinations in active layer still happen as the former case.

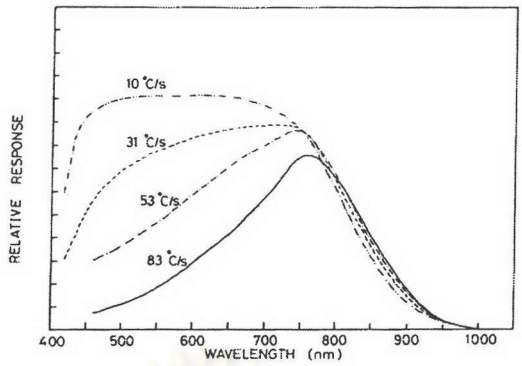

Fig. 5.8 Spectral response of RTD photodiodes as a function of the heating rate with the hold time of 9 sec at diffusion temperatures [23]

Up to this point, we realize that the thin staircase bandgap structure layers applied around metallurgical junction location of structure III does not have a strong influence in spectral response because the GaAs, which has higher absorption coefficient, plays an important roll for this particular characteristic. However, the $Ga_{1-x}Al_xAs$ staircase bandgap structure itself would benefit from the quasi-electric field both in conduction band and valence band as we have mentioned in chapter 3. Anyway, the best location of pn-junction is questionable hence we have designed the pn metallurgical junction with four different locations as depicted in Fig. 5.9 and each design has the band diagram as illustrated in Fig. 5.10, 5.11, 5.12 and 5.13 for location 1, 2, 3 and 4 respectively. The discussion will report on the following paragraphs.

Location 1 pn metallurgical junction

This design which the staircase bandgap layers behave as the window has no band edge discontinuities in active region. Therefore the EHPs which are almost generated in this region could only be separated by the external electric field toward the n side and p side.

Location 2 pn metallurgical junction

In this design, the band discontinuities occur both in conduction band and valence band and therefore the quasi-electric field for electrons and holes can be built. EHPs which are generated in active region can be separated and consequently swept toward the n-side and p-side and finally contribute to the drift current. Anyway, this design has the trouble with one recombination zone around the interface of $Ga_{0.9}Al_{0.1}As$ (N^-) and GaAs (n^-).

Location 3 pn metallurgical junction

In this design, the pn junction is located between $Ga_{0.7}Al_{0.3}As$ (P^+) and $Ga_{0.8}Al_{0.2}As$ (N^-), where is the interface between wider bandgap materials, the breakdown voltage is consequently higher. This design has the quasi-electric field as the one of location 2 therefore the carriers can be forced to sweep. The trouble is that the active region has two recombination zones.

Location 4 pn metallurgical junction

The breakdown voltage is higher comparing to the one of location 3 because its pn junction is between $Ga_{0.6}Al_{0.4}As$ (P^+) and $Ga_{0.7}Al_{0.3}As$ (N^-) where is the interface of wider bandgap. This design can perform as the one of location 3 except that the active region has the three recombination zones.

As a result, the best location of pn junction should be at location 3 or 4 to gain the higher breakdown voltage. In addition, the quasi-electric field can be optimized by adjusting the thickness "d" of these staircase bandgap $Ga_{1-x}Al_xAs$ layers, as depicted in Fig. 5.12 and 5.13, as well as their doping concentration.

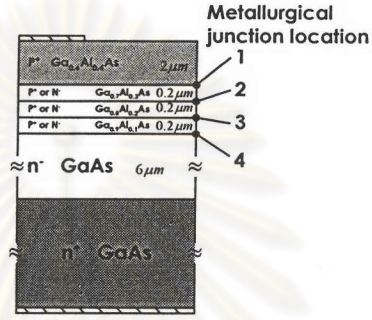

Fig. 5.9 Staircase bandgap around pn metallurgical junction

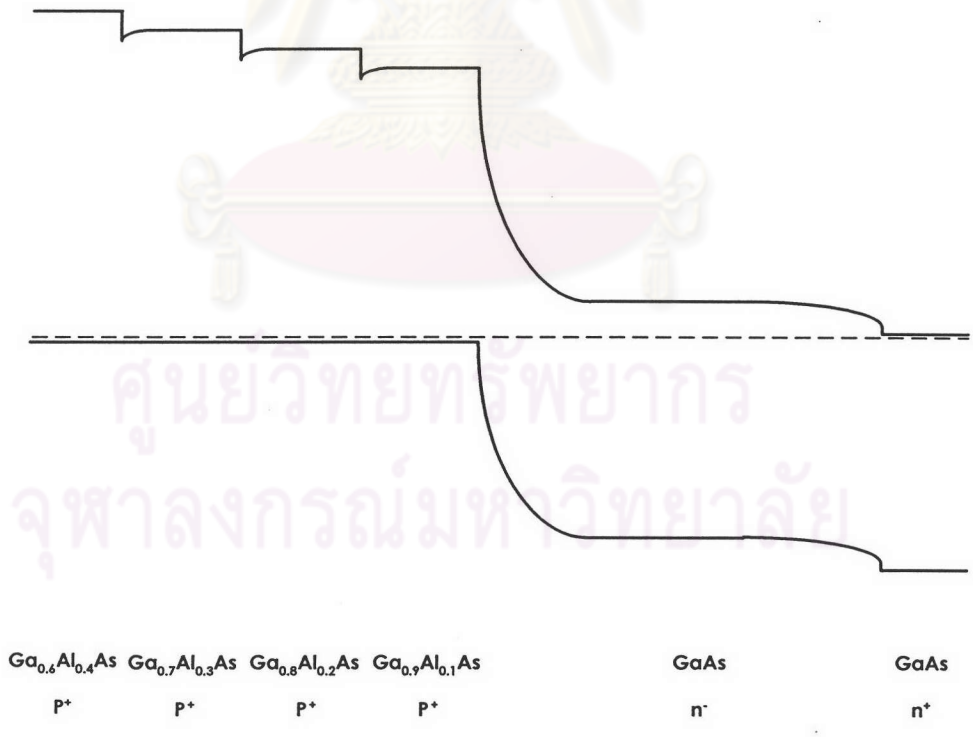

Fig. 5.10 Band diagram of staircase bangap photodiode with location 1 metallurgical junction

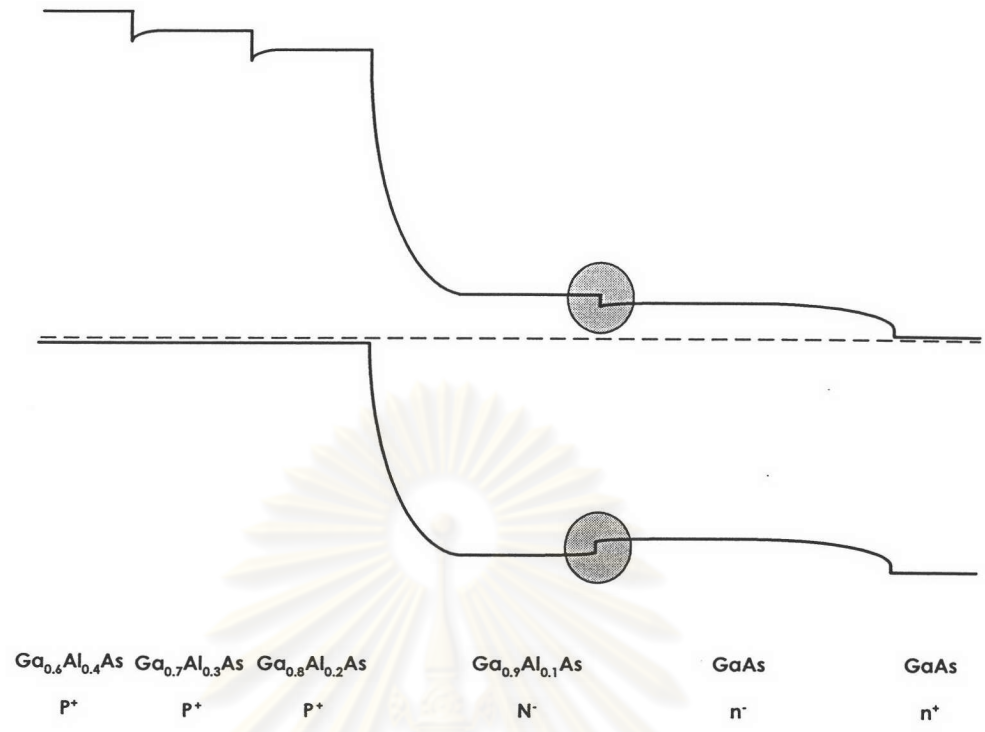

Fig. 5.11 Band diagram of staircase bangap photodiode with location 2 metallurgical Junction

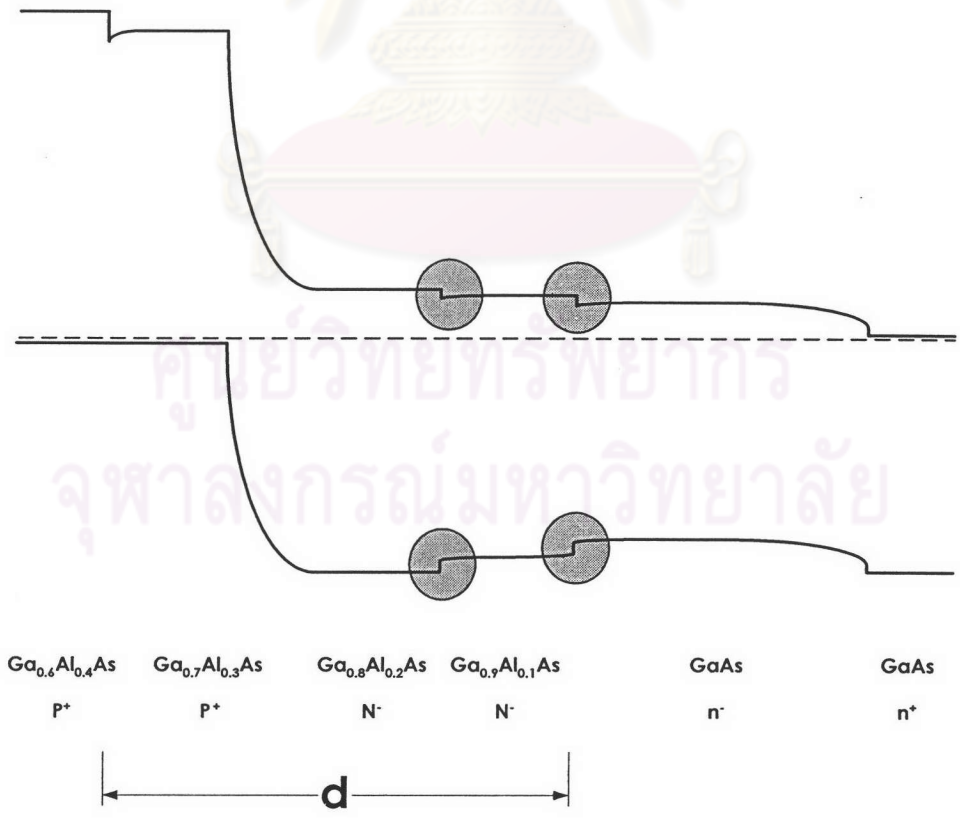

Fig. 5.12 Band diagram of staircase bangap photodiode with location 3 metallurgical junction

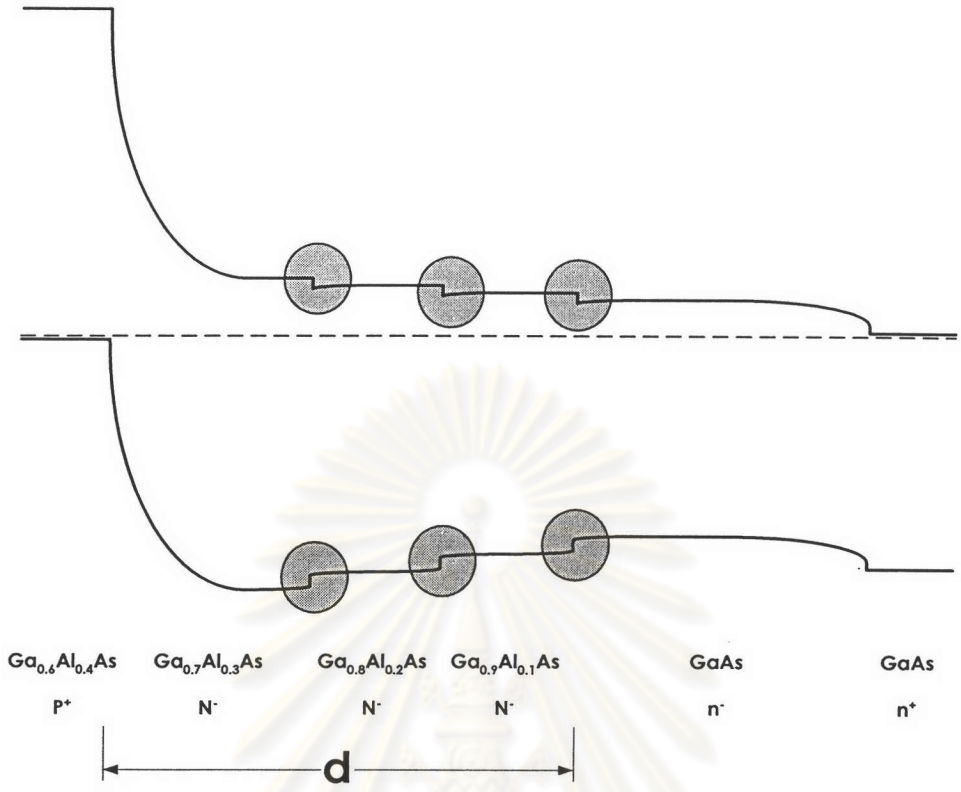

Fig. 5.13 Band diagram of staircase bangap photodiode with location 4 metallurgical junction